

# Non-Natural Cell Surface Receptors: Synthetic Peptides Capped with N-Cholesterylglycine Efficiently Deliver Proteins into Mammalian Cells

Scott E. Martin and Blake R. Peterson\*

Department of Chemistry, The Pennsylvania State University, 152 Davey Lab, University Park, Pennsylvania 16802. Received September 5, 2002; Revised Manuscript Received October 9, 2002

Protein toxins such as shiga toxin and cholera toxin penetrate into cells by binding small molecule-based cell surface receptors localized to cholesterol and sphingolipid-rich lipid raft subdomains of cellular plasma membranes. Molecular recognition between these toxins and their receptors triggers endocytic protein uptake through endogenous membrane trafficking pathways. We report herein the synthesis of functionally related non-natural cell surface receptors comprising peptides capped with N-cholesterylglycine as the plasma membrane anchor. The peptide moieties of these receptors were based on high-affinity epitopes of anti-hemagglutinin antibodies (anti-HA), anti-Flag antibodies, and a moderate-affinity *Strep* Tag II peptide ligand of the streptavidin protein from *Streptomyces avidini*. These non-natural receptors were directly loaded into plasma membranes of Jurkat lymphocytes to display peptides from lipid rafts on the cell surface. Molecular recognition between these receptors and added cognate anti-HA, anti-Flag, or streptavidin proteins resulted in rapid clathrin-mediated endocytosis; fluorescent target proteins were completely internalized within 4–12 h of protein addition. Analysis of protein uptake by epifluorescence microscopy and flow cytometry revealed intracellular fluorescence enhancements of 100-fold to 200-fold (10  $\mu$ M non-natural receptor) with typically >99% efficiency. This method enabled intracellular delivery of a functional *Escherichia coli*  $\beta$ -galactosidase enzyme conjugated to Protein A from *Staphylococcus aureus*. We termed this novel delivery strategy “synthetic receptor targeting”, which is an efficient method to enhance macromolecular uptake by decorating mammalian cells with chemically defined synthetic receptors that access the molecular machinery controlling the organization of cellular plasma membranes.

## INTRODUCTION

The hydrophobic character of cellular plasma membranes effectively seals the inner machinery of cells away from many molecules in the extracellular environment. Typically only moderately hydrophobic compounds of low molecular weight undergo rapid passive diffusion across low-polarity cellular membranes; macromolecules such as proteins and DNA generally require specific active transport mechanisms to access the cell interior (1). To circumvent this obstacle, many methods have been developed to enhance the cellular uptake of poorly permeable molecules (2–9). Many such methods involve covalent or noncovalent modification of macromolecules with polymers, lipids, or other agents that favorably alter the chemical properties of macromolecular cargo. In particular, peptides that mediate membrane translocation comprise an important class of oligomeric delivery vectors (2). However, the molecular mechanisms underlying many cellular delivery systems are not yet well enough understood to consistently and efficiently deliver macromolecules to desired targets in diverse cell lines. Hence, improved delivery systems with well-defined molecular mechanisms of action are needed in basic cell biology, tumor therapy, and genetic therapy.

Mammalian cells internalize nutrients and other macromolecular entities through the active transport mechanism of endocytosis (10, 11). This mechanism typically

involves recognition of molecules by plasma-membrane-associated receptors, clustering of receptor–ligand complexes, and invagination of these regions of the plasma membrane to form intracellular vesicles. These vesicles fuse to form organelles termed endosomes that are directed to compartments for degradation or recycling of internalized contents. Under certain conditions, endosomal contents can also be released into the cytosol (10, 11). Endocytosis is a mechanism of cellular penetration employed by many viruses and toxins such as shiga toxin from *Shigella dysenteriae* and cholera toxin from *Vibrio cholerae* (12). These toxins are members of the AB<sub>5</sub> family of protein toxins (13) that penetrate into mammalian cells by binding of the toxin to small molecule cell surface receptors such as the glycosphingolipid Gb3 (shiga toxin receptor) and ganglioside GM1 (cholera toxin receptor). These low molecular weight receptors are sphingolipids that comprise tri- or pentasaccharide headgroups linked to the lipid ceramide (N-acyl sphingosine). These receptors reside in sphingolipid-rich lipid raft subdomains of cellular plasma membranes. Lipid rafts are composed of cholesterol packed with sphingolipids in a liquid ordered phase (14–17), and these subdomains are key elements involved in the control of numerous signal transduction pathways (18). Although both shiga toxin and cholera toxin penetrate into cells (12) primarily through the mechanism of clathrin-mediated endocytosis (19), the precise interactions that link these toxins to clathrin through their receptors and the role played by lipid rafts in this process are not yet well understood (20, 21).

\* Corresponding author. Email: brpeters@chem.psu.edu. Tel: (814) 865-2969. Fax: (814) 863-8403.

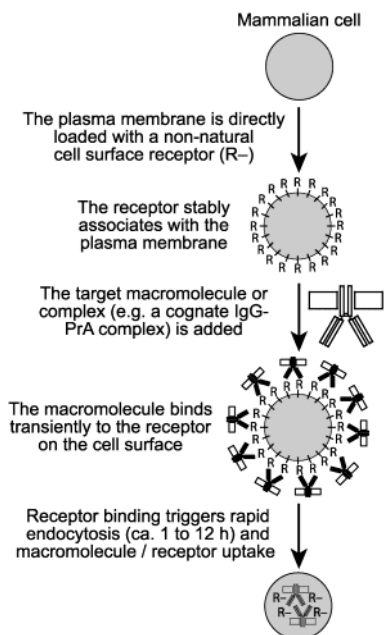


**Figure 1.** Delivery of macromolecules to cells by synthetic receptor targeting. Non-natural cell surface receptors directly loaded into cellular plasma membranes enable delivery of cognate macromolecules through endogenous membrane trafficking pathways.

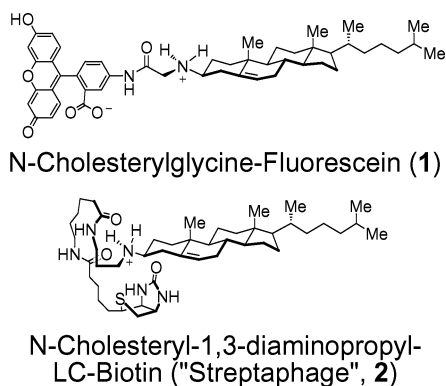


**Figure 2.** Structures of previously reported non-natural cell surface receptors.

Our laboratory is investigating a novel macromolecular delivery system termed here as "synthetic receptor targeting" (Figure 1). This method employs non-natural cell surface receptors such as compounds **1** and **2** (Figure 2) based on lipids that insert into cellular plasma membranes. These receptors comprise derivatives of  $3\beta$ -cholesterylamine linked to protein-binding motifs including fluorescein (22) and biotin (23). These compounds functionally mimic natural small-molecule receptors such as glycosphingolipid Gb3 or ganglioside GM1 by persistently associating with lipid raft subdomains of cellular plasma membranes. For example, the cholesterylamine-derived fluorescent probe **1** is primarily plasma-membrane-associated even 16 h after addition to living cells (22). However, as shown in Figure 1, binding of cognate proteins such as immunoglobulins (IgGs) or streptavidin to these plasma membrane-anchored small molecules rapidly triggers clathrin-mediated endocytosis of the receptor-protein complex (22, 23). This approach is conceptually related to elegant studies of metabolic cell surface engineering that display non-natural functional groups such as ketones and azides on cell surfaces (24–27). These ketones and other functional groups can

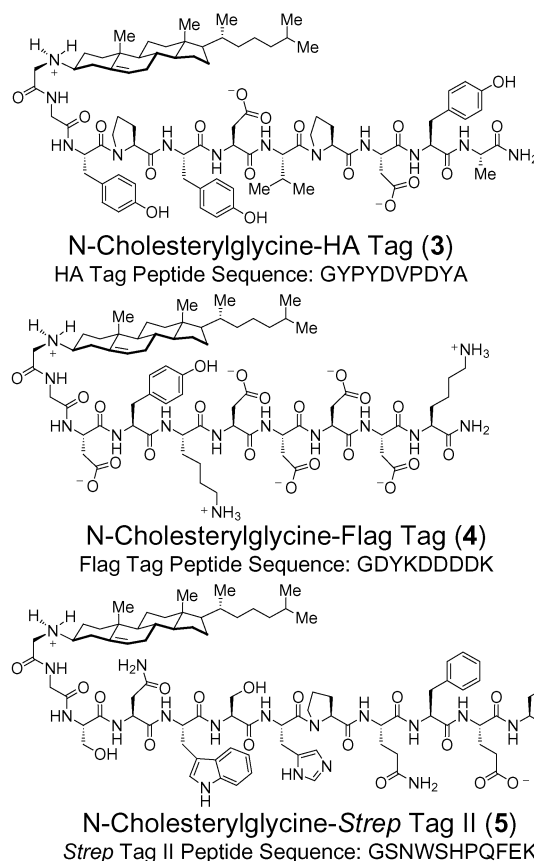


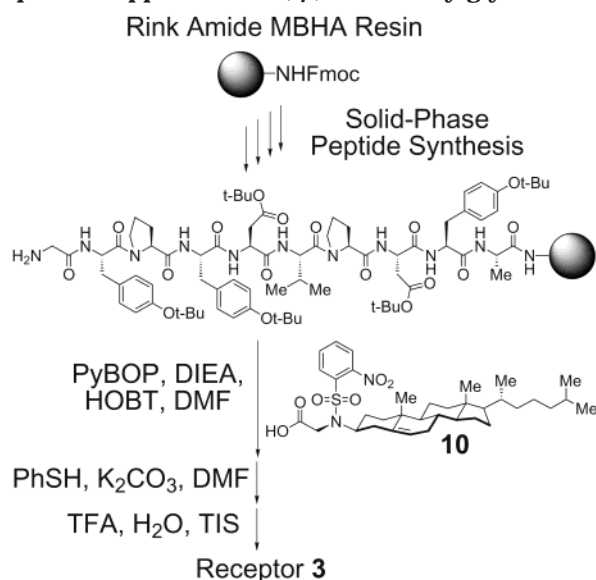
**Figure 3.** Structures of non-natural receptors based on N-( $3\beta$ )-cholesteryl-glycine-capped peptides.

be incorporated into diverse glycolipids and glycoproteins on cells by accessing endogenous pathways of oligosaccharide biosynthesis with engineered monosaccharide precursors (28–30).

We describe here three novel non-natural small-molecule receptors (Figure 3, **3**–**5**) that deliver proteins into Jurkat lymphocytes. These receptors comprise protein-binding peptides capped with N-cholesteryl-glycine. As shown in Figure 3, peptide derivatives **3** and **4** are membrane-anchored antigens designed to bind commercially available anti-hemagglutinin (anti-HA) and anti-Flag IgGs. Peptide **5** is a derivative of the previously reported *Strep* Tag II peptide, which is a ligand of the streptavidin protein from *Staphylococcus aureus* (31). We report that receptors **3**–**5** dramatically enhance endocytic uptake of cognate proteins by mammalian cells, and this approach can deliver functional enzymes such as  $\beta$ -galactosidase conjugated to Protein A from *Staphylococcus aureus*.

## EXPERIMENTAL PROCEDURES

**General.** Chemical reagents and solvents were obtained from Aldrich, Alfa Aesar, Fluka, or VWR Scientific. Media and antibiotics were obtained from Gibco BRL. Streptavidin Alexa Fluor 488 (SA488), Cholera toxin Alexa Fluor 594, Protein A Alexa Fluor 488 (PrA488), and Lysotracker Red were purchased from Molecular Probes. Protein A- $\beta$ -galactosidase (PrA- $\beta$ -Gal), chlorpromazine, sucrose, methyl- $\beta$ -cyclodextrin, rabbit anti-Flag IgG, and rabbit anti-HA IgG were obtained from Sigma. Fmoc-protected amino acids, coupling reagents, and Rink Amide MBHA resin (75–150  $\mu$ m, 0.7 mmol/g) were purchased from Novabiochem. Analytical and semipreparative HPLC analysis/purifica-

**Scheme 1. General Strategy for Synthesis of Peptides Capped with N-(3 $\beta$ )-Cholesterylglycine**


tion employed a Hewlett-Packard HP 1100 instrument with StableBond C18 columns (analytical column: 300 SB-C18, 4.6 mm  $\times$  25 cm, 1 mL/min flow rate; semi-preparative column: 300 SB-C18, 9.4 mm  $\times$  25 cm, 3 mL/min flow rate) using a gradient from 9:1:0.001 ddw/CH<sub>3</sub>CN/TFA to 0.9:9.1:0.001 ddw/CH<sub>3</sub>CN/TFA over 40 min. Peptide mass spectrometry was obtained on a Perseptive Voyager DE-STR MALDI-TOF instrument. Epifluorescence micrographs were captured through a Zeiss Fluor (100 $\times$ ) objective by a Zeiss Axiocam digital camera interfaced to a Zeiss Axiovert S100TV microscope. Images were processed with Adobe Photoshop 5.0.

**Control and Fluorescent Peptides.** Two peptides were synthesized as C-terminal carboxamides to provide nonmembrane binding competitors. Peptide **6** sequence, YPYDVPDYA; peptide **7**, GDYKDDDDK. Biotin provided the soluble streptavidin competitor. Two peptides were synthesized as C-terminal carboxamides for fluorescence polarization assays. Peptide **8**, Fluor-GYPYDVPDYA; peptide **9**, Fluor-GDYKDDDDK. Fluor = fluorescein-5(6)-carboxamidohexanoamide. Peptide sequences are listed in single letter amino acid codes.

**Peptide Synthesis.** Peptides were synthesized with an Advanced Chemtech FBS-357 automated batch-mode synthesizer. Peptide synthesis employed standard N $\alpha$ -Fmoc methodology with *tert*-butyl ester, *tert*-butyl ether, *tert*-butyl carbamate, and methyltrityl side chain protection. Deprotection of Fmoc carbamates on Rink Amide MBHA resin (50 mg, 35  $\mu$ mol) was effected by the addition of 30% piperidine in DMF (2  $\times$  1 mL for 5 min followed by 1 mL for 20 min). N $\alpha$ -Fmoc amino acids were coupled as previously described (32). Peptide precursors to **3–5** were capped with the cholesteryl moiety by coupling with the nosyl-protected N-(3 $\beta$ )-cholesterylglycine (**10**, Scheme 1) prepared as previously reported (22). Peptides were capped with **10** by sequential addition of the following reagents in DMF: **10**/HOBT (250  $\mu$ L, 0.5 M of each component), followed by PyBOP (250  $\mu$ L, 0.5 M) and DIEA (500  $\mu$ L, 0.5 M). The resin was subsequently agitated for 1 h at 23  $^{\circ}$ C. This coupling step was repeated, and all amines were acylated as evidenced by Kaiser test. Deprotection of the nosyl sulfonamide was effected by treatment with K<sub>2</sub>CO<sub>3</sub> (70 mg) and thiophenol (25 mg) in DMF (2 mL) for 16 h. Fluorescent peptides **8** and **9** were synthesized with 23 mg of Rink Amide MBHA

**Table 1. Analytical Data for Peptides 3–9**

| peptide, formula                                                            | yield | M + H <sub>calcd</sub> | M + H <sub>obs</sub> |
|-----------------------------------------------------------------------------|-------|------------------------|----------------------|
| <b>3</b> , C <sub>84</sub> H <sub>118</sub> N <sub>12</sub> O <sub>18</sub> | 15%   | 1583.9                 | 1583.9               |
| <b>4</b> , C <sub>72</sub> H <sub>111</sub> N <sub>13</sub> O <sub>21</sub> | 19%   | 1494.8                 | 1494.8               |
| <b>5</b> , C <sub>88</sub> H <sub>129</sub> N <sub>19</sub> O <sub>18</sub> | 23%   | 1741.0                 | 1741.0               |
| <b>6</b> , C <sub>53</sub> H <sub>68</sub> N <sub>10</sub> O <sub>16</sub>  | 58%   | 1101.5                 | 1101.5               |
| <b>7</b> , C <sub>43</sub> H <sub>64</sub> N <sub>12</sub> O <sub>20</sub>  | 59%   | 1069.4                 | 1069.4               |
| <b>8</b> , C <sub>82</sub> H <sub>92</sub> N <sub>12</sub> O <sub>24</sub>  | 42%   | 1629.7                 | 1629.6               |
| <b>9</b> , C <sub>70</sub> H <sub>85</sub> N <sub>13</sub> O <sub>27</sub>  | 20%   | 1540.6                 | 1540.6               |

resin (16  $\mu$ mol). After N $\alpha$ -Fmoc deprotection of the N-terminal amino acid of resin-bound precursors to peptides **8** and **9**, fluorescein-5(6)-carboxamidohexanoic acid succinimidyl ester (12 mg, 24  $\mu$ mol in 500  $\mu$ L of DMF) and DIEA (500  $\mu$ L, 0.5 M in DMF) were added with shaking for 16 h at 23  $^{\circ}$ C. Cleavage of peptides from the resin and side chain deprotection employed TFA/H<sub>2</sub>O/TIS (1 mL, 95:2.5:2.5) for 1 h. Peptides were purified by reverse-phase HPLC to >90% homogeneity, and peptides were analyzed by MALDI-TOF mass spectrometry as shown in Table 1.

**Flow Cytometry.** Analyses were performed with a Beckman-Coulter XL-MCL benchtop flow cytometer equipped with a 15 mW air-cooled argon-ion laser. Fluorescence detection was derived from excitation at 488 nm, splitting the emission with a 550 nm dichroic and long pass filter, and optical filtering through 530/30-nm band-pass filter. Forward-scatter (FS) and side-scatter (SSC) dot plots afforded cellular physical properties of size and granularity that allowed gating of living cells. After gating, 10 000 cells were counted.

**Confocal Microscopy.** Sequential scans were performed on an Olympus FV300 laser scanning confocal microscope fitted with a UplanFl objective (100 X). Alexa Fluor 488 was excited with a 488 nm Argon ion laser, and emitted photons were collected through 510 nm LP and 530 nm SP filters. Excitation of Alexa Fluor 594 employed a 543 nm HeNe laser and a 605 nm BP filter.

**Antibody Uptake Assays.** Human Jurkat T lymphocytes were maintained in Roswell Park Memorial Institute (RPMI) 1640 media supplemented with Fetal Bovine Serum (FBS, 10%), penicillin (100 units/mL), and streptomycin (100  $\mu$ g/mL). Receptors **3–5** were dissolved in dimethyl sulfoxide (DMSO), which was diluted with media to yield a final DMSO concentration of 1%. For antibody/PrA488 uptake assays, Jurkat cells (5  $\times$  10<sup>6</sup>) were incubated with receptors **3–5** at 37  $^{\circ}$ C for 1 h, washed with media (2  $\times$  0.5 mL), and resuspended in media (490  $\mu$ L). To these cells was added a mixture of antibody (2.7  $\mu$ g) and PrA488 (0.5  $\mu$ g) in phosphate buffered saline (PBS, 10  $\mu$ L, pH 7.4). This protein mixture was preincubated at 23  $^{\circ}$ C for 1 h prior to addition to cells. Cells were maintained at 37  $^{\circ}$ C for 12 h. Cells were then washed with media (1  $\times$  0.5 mL), incubated with the appropriate free peptide (100  $\mu$ M, **6** or **7**) in media (2  $\times$  0.5 mL  $\times$  30 min) to compete away any noninternalized protein, washed with media (1  $\times$  0.5 mL), resuspended in media (0.75 mL), and analyzed by flow cytometry.

**Cellular Uptake of Protein A- $\beta$ -Galactosidase (PrA- $\beta$ -Gal).** The antibody/PrA- $\beta$ -Gal uptake assays employed Jurkat cells (5  $\times$  10<sup>6</sup>) incubated with receptor **3** (10  $\mu$ M) at 37  $^{\circ}$ C for 1 h. The cells were washed with media (2  $\times$  0.5 mL) and resuspended in media (490  $\mu$ L). A mixture of rabbit anti HA antibody (2.7  $\mu$ g) and PrA- $\beta$ -Gal (4  $\mu$ L, 0.3 units) in PBS (10  $\mu$ L, pH 7.4) was incubated at 23  $^{\circ}$ C for 1 h and then added to the cells treated with **3**. Cells were maintained at 37  $^{\circ}$ C for 12 h, washed with media (1  $\times$  0.5 mL), and incubated with free

HA peptide in media ( $100\ \mu\text{M}$ ,  $3 \times 0.5\ \text{mL} \times 30\ \text{min}$ ) to competitively displace any plasma membrane-bound protein. Uptake of PrA- $\beta$ -Gal was detected by incubation with fluorescein di- $(\beta$ -D-galactopyranoside) in media ( $1\ \text{mM}$ , 2% DMSO) for 30 min at  $37\ ^\circ\text{C}$ . After this incubation, cells were washed with media ( $1 \times 1\ \text{mL}$ ), resuspended in media ( $0.75\ \text{mL}$ ), and analyzed by flow cytometry.

**Streptavidin Uptake Assay.** Receptors **3–5** were dissolved in DMSO and diluted with media to yield a final DMSO concentration of 1%. Jurkat cells ( $5 \times 10^6$ ) were incubated with receptors **3–5** at  $37\ ^\circ\text{C}$  for 1 h, washed with media ( $2 \times 0.5\ \text{mL}$ ), and resuspended in media ( $198\ \mu\text{L}$ ). To these cells was added streptavidin Alexa Fluor 488 (SA 488,  $2\ \mu\text{g}$ ), and cells were maintained at  $37\ ^\circ\text{C}$  for 4 h. Cells were washed with media ( $1 \times 0.5\ \text{mL}$ ), followed by media containing biotin ( $50\ \mu\text{M}$ , 1% DMSO,  $2 \times 0.5\ \text{mL}$ ) as a nonmembrane binding competitor to displace any noninternalized protein. The cells were washed again with media ( $1 \times 0.5\ \text{mL}$ ) and resuspended in media ( $0.75\ \text{mL}$ ) for analysis by flow cytometry.

**Inhibition of Uptake Experiments.** Receptor **3** ( $1\ \mu\text{M}$ ) was subjected to the uptake assay with an antibody/PrA 488 incubation time of 4 h.

**Depletion of Cellular Cholesterol with Methyl- $\beta$ -Cyclodextrin (CD).** Cells were suspended in PBS (pH 7.4) containing BSA ( $1\ \text{mg/mL}$ ) and CD ( $10\ \text{mM}$ ) for 30 min prior to the protein uptake assay, and BSA ( $1\ \text{mg/mL}$ ) was included in subsequent assay media.

**Treatment with Hypertonic Sucrose.** Cells were suspended in media containing sucrose ( $400\ \text{mM}$ ) for 1 h prior to the protein uptake assay, and sucrose ( $400\ \text{mM}$ ) was included in subsequent assay media.

**Treatment with Chlorpromazine.** Cells were suspended in media containing chlorpromazine ( $100\ \mu\text{M}$ ) for 1 h prior to the protein uptake assay, and chlorpromazine ( $100\ \mu\text{M}$ ) was included in subsequent assay media.

**Fluorescence Polarization Assays.** Apparent binding constants for rabbit anti-HA and anti-Flag IgGs were determined by fluorescence polarization measurements with a Packard Fusion microtiterplate reader utilizing a 485 nm excitation filter and a 535 nm fluorescence polarization emission filter. All fluorescence polarization experiments employed black 384 well plates (Costar) with a fixed concentration of **8** or **9** ( $10\ \text{nM}$ ) in PBS (pH 7.4,  $40\ \mu\text{L}$ ). Fluorescent peptides **8** and **9** were equilibrated with cognate antibodies for 10 min prior to fluorescence polarization measurements. Dissociation constants were calculated by nonlinear regression with a one-site binding model (GraphPad Prism 3 software). Errors reflect calculated standard errors of the mean.

## RESULTS AND DISCUSSION

**Design and Synthesis of Non-Natural Cell Surface Receptors.** Receptors **3** and **4** were designed on the basis of known short peptide epitopes of anti-HA (epitope sequence: YPYDVPDYA) (*33*) and anti-Flag (epitope sequence: DYKDDDDK) IgGs (*34*). Receptor **5** was designed from the previously reported *Strep* Tag II peptide (sequence: SNWSHPQFEK), which is a moderate affinity ( $K_d = 72\ \mu\text{M}$ ) peptide ligand of the protein streptavidin (SA) (*31*).

To examine hypothetical geometries of receptors **3** and **5** bound to cognate proteins, models of molecular complexes interacting with a model membrane were constructed (Figure 4). These models employed X-ray crystal structures of a peptide-bound anti-HA fab fragment

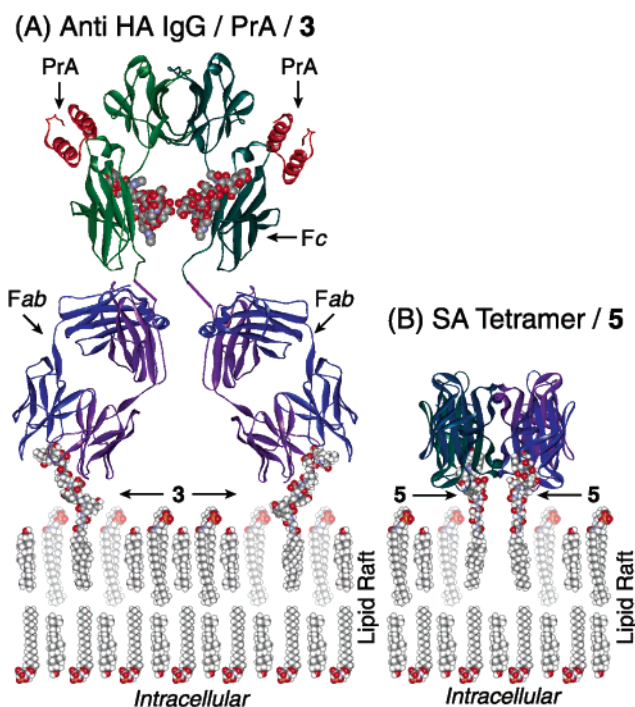


**Figure 4.** Molecular models of proteins (ribbon diagrams) bound to Macromodel-minimized peptidic receptors (CPK models) inserted into a model lipid raft (CPK models). (A) Model of anti-HA/PrA bound to **3**. (B) Model of SA bound to **5**.

(PDB# 1FRG) (*33*) and *Strep* Tag II-bound SA (PDB# 1KL5) (*35*). The anti-HA model was embellished by inclusion of the invariant Fc fragment from an X-ray structure of IgG2a (PDB# 1IGT) (*36*) and the structure of a Fc-bound fragment of PrA (PDB# 1FC2) (*37*). Model construction involved modification of the X-ray structure of the anti-HA epitope peptide and the SA-bound *Strep* Tag II peptide by addition of a flexible glycine residue appended to the peptide N-terminus, which was further capped with N-( $3\beta$ )-cholesteryl-glycine (*22*). The model cholesteryl-glycine-Gly moiety was minimized with the Macromodel (v. 6.5) (*38*) Amber\* force field prior to attachment to the bound peptide ligands of cognate proteins (Figure 4). WebLab ViewerLite (Molecular Simulations Inc., v. 3.2) was employed to display the complexes. The model membrane bilayer was constructed to mimic the composition of a lipid raft subdomain composed of cholesterol packed with sphingomyelin in the outer leaflet and cholesterol packed with saturated phosphatidylserine in the inner leaflet (Figure 4) (*17*). These modeling studies suggested that a glycine linker between the protein-bound peptides and N-( $3\beta$ )-cholesteryl-glycine would be sufficient to enable complete insertion of the bound steroid into the model membrane. The length of linker between the steroid and protein ligand has been shown to be critical in structurally related systems (*23*).

Receptors **3–5** were synthesized as shown in Scheme 1. The peptide precursors were synthesized and capped with a previously reported nosyl-protected N-( $3\beta$ )-cholesteryl-glycine (**10**) (*22*). The nosyl protecting group was removed on solid phase with deprotonated thiophenol prior to cleavage of peptides from the solid support. Analogous control peptides **6** and **7** were synthesized lacking the N-cholesteryl-glycine moiety to serve as non-membrane binding competitors. Because the affinities of rabbit anti-HA and rabbit anti-Flag IgGs have not been previously reported, fluorescent peptides **8** and **9** were

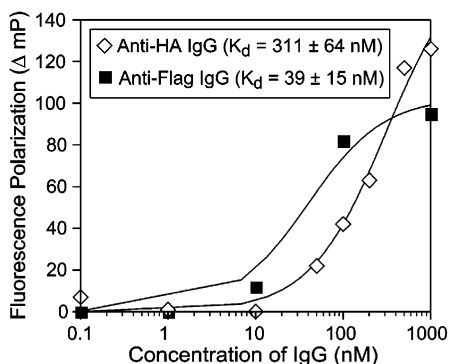


**Figure 5.** Determination of apparent dissociation constants ( $K_d$ ) of anti-HA and anti-Flag IgGs by quantification of the fluorescence polarization of peptides **8** and **9**.

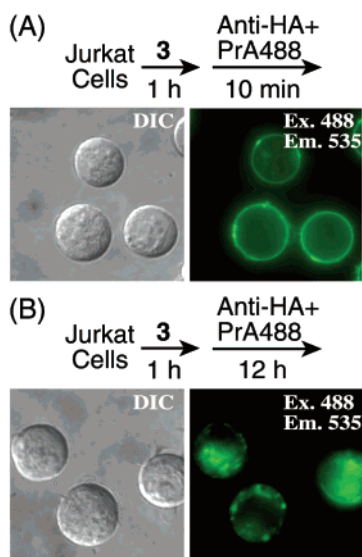


**Figure 6.** Differential interference contrast (DIC) and epifluorescence micrographs of Jurkat lymphocytes treated with receptor **3** ( $10 \mu\text{M}$ ), anti-HA, and green fluorescent PrA488. Fluorescence excitation (Ex.) and emission (Em.) wavelengths (nm) are explicitly shown.

synthesized as analogues of **3** and **4** that substitute the N-cholesteryl-glycine moiety with a fluorescein derivative to enable determination of peptide affinities by fluorescence polarization (FP) measurements (39). As shown in Figure 5, quantification of FP values as a function of IgG concentration yielded apparent  $K_d$  values of  $311 \pm 64 \text{ nM}$  for the anti-HA-binding peptide **8** and  $39 \pm 15 \text{ nM}$  for the anti-Flag-binding peptide **9**. In these experiments, the concentration of the fluorescent tracer peptide was fixed at  $10 \text{ nM}$ .

**Uptake of Proteins by Mammalian Cells Bearing Non-Natural Cell Surface Receptors.** Initial qualitative analysis of protein uptake mediated by receptors **3**–**5** employed epifluorescence microscopy. As shown in Figure 6, Jurkat lymphocytes treated with receptor **3** for 1 h followed by addition of anti-HA and green fluorescent PrA (PrA488) as a probe exhibited bright fluorescence at the cellular periphery within 10 min of protein addition. This peripheral fluorescence was localized to the plasma membrane of practically 100% of viable cells as compared with fluorescent plasma membrane probes such as the fluorescent analogue **1** (22, 40). After 12 h of protein treatment, the fluorescence was observed in defined compartments in the cell interior, indicating that the protein complex was internalized (Figure 6). Cells treated with receptor **4** followed by anti-Flag IgG/PrA488 or

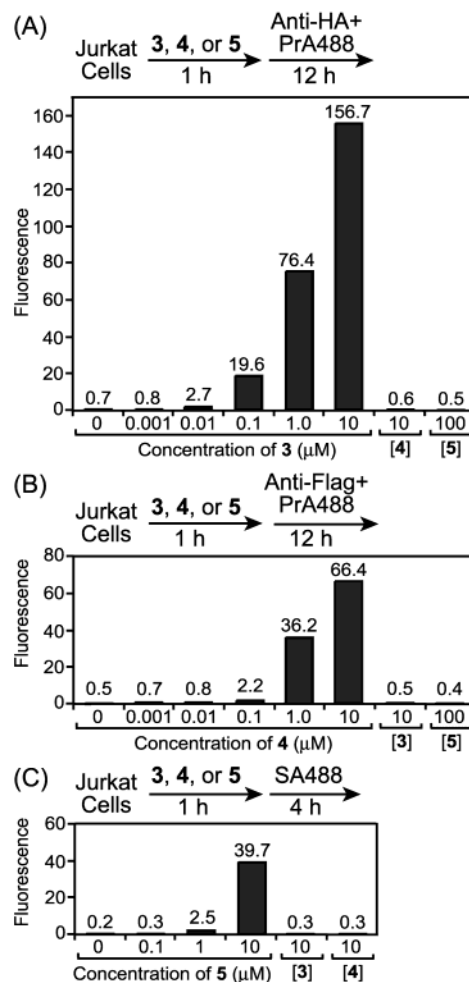


**Figure 7.** Analysis of dose-dependent cellular uptake of proteins by flow cytometry. Each bar represents the median fluorescence of 10 000 living cells.

treated with receptor **5** followed by SA488 showed highly similar patterns of cellular fluorescence (data not shown).

To quantitatively examine this uptake process, dose-dependent effects on intracellular fluorescence were measured by flow cytometry. Because flow cytometry cannot distinguish membrane-associated from intracellular fluorescence, cells were extensively washed with soluble competitor peptides ( $100 \mu\text{M}$ ) or biotin ( $50 \mu\text{M}$ ) prior to analysis to displace any noninternalized protein. As shown in Figure 7A, pretreatment of cells with **3** for 1 h followed by addition of anti-HA and PrA488 for 12 h dramatically enhanced intracellular fluorescence with significant effects observed at concentrations of **3** as low as  $100 \text{ nM}$ . The intracellular fluorescence of cells pretreated with  $10 \mu\text{M}$  **3** was enhanced by over 200-fold compared with cells treated with the anti-HA/PrA488 complex alone. This effect on anti-HA/PrA488 specifically required receptor **3**; no uptake of this complex was mediated by receptors **4** or **5** (Figure 7A). However, receptor **4** efficiently and specifically mediated the dose-dependent uptake of anti-Flag/PrA488 with over a 100-fold enhancement of intracellular fluorescence at  $10 \mu\text{M}$  (Figure 7B). Furthermore, green fluorescent streptavidin (SA488) was specifically internalized by receptor **5**, which enhanced uptake by over 100-fold at  $10 \mu\text{M}$  (Figure 7C).

**Non-Natural Cell Surface Receptors Direct Cognate Proteins to Lipid Rafts and Effect Protein Uptake via Clathrin-Mediated Endocytosis.** The biotin-derived “streptaphage” receptor (**2**) was previously

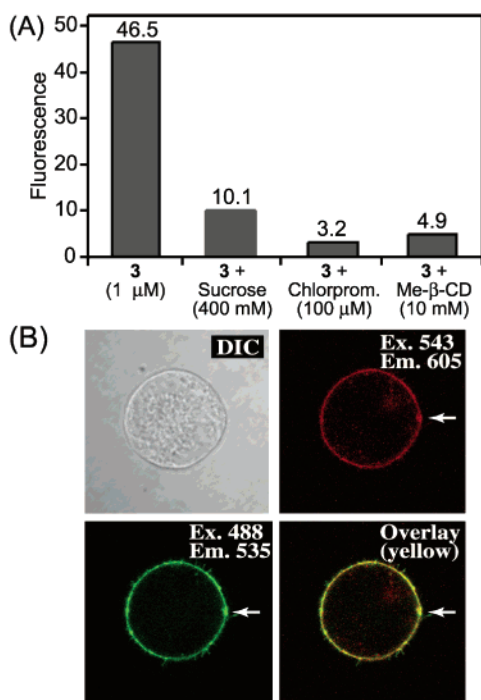


**Figure 8.** Analysis of inhibition of protein uptake and protein subcellular localization. (A) Uptake of anti-HA/PrA488/3 measured by flow cytometry in the presence of inhibitors of clathrin-mediated endocytosis. (B) Confocal laser scanning microscopy of cells treated with **3** for 1 h followed by anti-HA/PrA488 and red fluorescent Alexa fluor-594 Cholera toxin B subunit for 5 min. White arrows illustrate colocalization of green and red fluorescence.

shown to mediate uptake of streptavidin by targeting this protein to lipid rafts and promoting clathrin-mediated endocytosis (23). To examine the mechanism of uptake of structurally related receptors **3–5**, protein uptake under conditions that block clathrin-mediated endocytosis was examined (Figure 8A). Cells treated with hypertonic sucrose exhibit defects in clathrin-coated lattices (41), and these conditions were found to diminish receptor **3**-mediated uptake of anti-HA/PrA488 measured by flow cytometry. In addition, the cationic amphiphatic drug chlorpromazine disrupts the assembly/disassembly of clathrin associated with coated pits and endosomes (42), and this drug inhibited protein uptake. Furthermore, depletion of cellular cholesterol by treatment with methyl- $\beta$ -cyclodextrin to disrupt lipid rafts (43) blocked protein uptake. These results indicate that lipid rafts may be important for this process, and protein uptake mediated by receptors **3–5** is most likely controlled by a clathrin-mediated endocytosis mechanism.

To examine the localization of proteins binding to non-natural receptors in cellular plasma membranes, cells were treated with **3** followed by addition of anti-HA/PrA488 and red fluorescent cholera toxin B subunit. Cholera toxin binds ganglioside GM1 in lipid rafts and provides a probe of these membrane subdomains. As shown in Figure 8B, confocal laser scanning microscopy revealed a heterogeneous distribution of anti-HA/PrA488/3 in plasma membranes of Jurkat lymphocytes. Moreover, this complex extensively colocalized with cholera toxin, indicating that receptor **3** mediates protein association with lipid rafts.

**Non-Natural Receptor-Mediated Delivery of Functional  $\beta$ -Galactosidase into Cells.** Functional enzymes such as caspases (9), ribonuclease (44), and horseradish peroxidase (45) have been delivered into cells by a variety

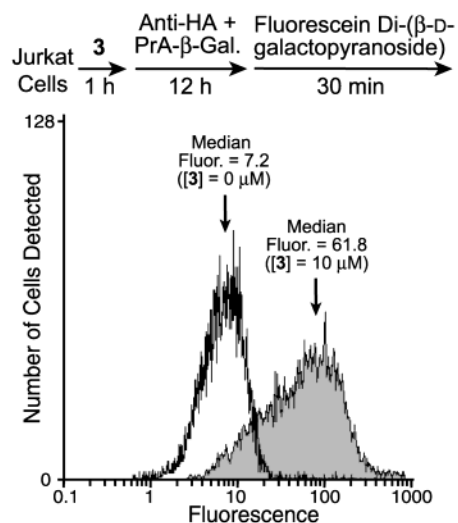


**Figure 9.** Flow cytometry of Jurkat lymphocytes treated with receptor **3**, anti-HA IgG, and PrA- $\beta$ -galactosidase.

of carrier mechanisms and are under investigation as components of antitumor agents. To investigate whether a synthetic cell surface receptor might enable delivery of a functional enzyme into mammalian cells, uptake of a commercially available Protein A- $\beta$ -galactosidase conjugate (PrA- $\beta$ -Gal) was examined. As shown in Figure 9, Jurkat lymphocytes were treated with receptor **3** and the anti-HA/PrA- $\beta$ -Gal conjugate. Cells were treated with a fluorescent substrate of  $\beta$ -galactosidase, and fluorescence was analyzed by flow cytometry. These experiments revealed that receptor **3** engendered a ca. 9-fold enhancement of median cellular fluorescence compared with identically treated cells in the absence of receptor **3**. Under these conditions, this fluorescence enhancement was detected in 75% of the treated cells (Figure 9). This result established that non-natural cell surface receptors such as **3** can deliver at least transiently functional enzymes into cells.

## CONCLUSION

We describe three novel non-natural cell surface receptors (**3–5**) that enable dose-dependent uptake of specific macromolecules by mammalian cells. These compounds comprise peptides capped with N-(3 $\beta$ )-cholesterylglycine, which is a mimic of cholesterol that can stably integrate into cellular plasma membranes of mammalian cells (22, 23). Addition of cognate IgGs or streptavidin proteins to cells displaying these non-natural cell surface receptors triggers endocytic protein uptake through endogenous membrane trafficking pathways.

Proteins delivered through this “synthetic receptor targeting” approach can span a wide range of affinities for non-natural cell surface receptors. For example streptavidin can be delivered to cells by surface display of either very high affinity biotin (100 fM) (23) or the modest affinity *Strep* Tag II peptide (receptor **5**, ca. 72  $\mu$ M). However, the magnitude of delivery of streptavidin is ca. 6.5-fold greater with the high-affinity biotin-derived receptor **2** compared with the modest-affinity receptor **5**. Despite these vast affinity differences, similarities in the magnitude of delivery may relate to the high effective concentration of non-natural receptors on cell surfaces and the multivalent nature of cell surface recognition by bivalent IgGs and tetrameric streptavidin. Interestingly, the higher affinity anti-Flag receptor **4** ( $K_d \sim 39\ \text{nM}$ ) delivered 2.4-fold less IgG/PrA complex than the lower

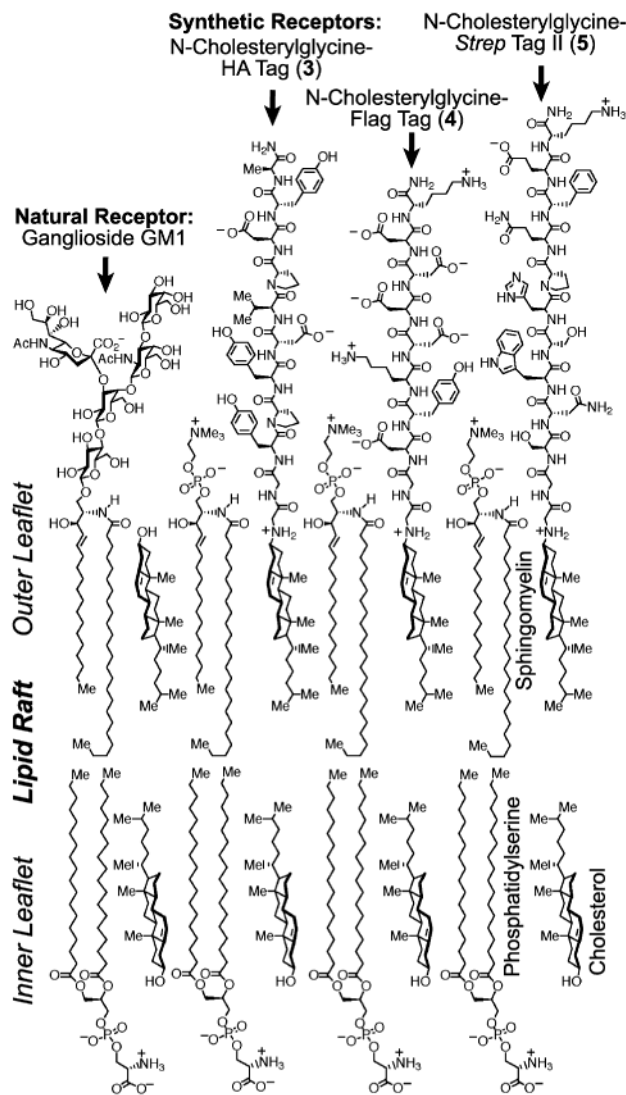


**Figure 10.** Model of a plasma membrane raft segment containing the non-natural receptors 3–5 and the natural receptor ganglioside GM1.

affinity anti-HA receptor 3 ( $K_d \sim 311$  nM). This result may relate to the highly acidic nature of the Flag epitope peptide, which has been shown to diminish the affinity of fusion proteins for cellular plasma membranes (34).

The non-natural receptors described herein appear to associate with lipid raft subdomains of cellular plasma membranes as evidenced by colocalization with cholera toxin on cell surfaces, and these receptors cause proteins to penetrate into cells by clathrin-mediated endocytosis. In this regard, as shown in a model of a lipid raft in Figure 10, these compounds functionally mimic natural cell surface receptors such as ganglioside GM1, which resides in lipid rafts and enables the cellular penetration of cholera toxin through endocytic uptake mechanisms. Given that non-natural cell surface receptors can be used for the delivery of functional enzymes of high molecular weight such as *E. Coli*  $\beta$ -galactosidase (tetramer  $\sim 540$  000 Da) (46) conjugated to Protein A ( $\sim 42$  000 Da) and bound to IgGs ( $\sim 150$  000 Da), this “synthetic receptor targeting” approach may have potential applications in tumor therapy by enabling the delivery of lethal enzymes into tumor cells. This approach may also facilitate studies in other areas requiring the delivery of macromolecules into mammalian cells including basic cell biology, genetic therapy, and immunology.

#### ACKNOWLEDGMENT

We thank the National Institutes of Health (RO1-CA83831) for financial support.

#### LITERATURE CITED

- (1) Smith, D. A.; van de Waterbeemd, H. *Curr. Opin. Chem. Biol.* **1999**, *3*, 373–378.
- (2) Fischer, P. M.; Krausz, E.; Lane, D. P. *Bioconjugate Chem.* **2001**, *12*, 825–841.
- (3) Garnett, M. C. *Crit. Rev. Ther. Drug Carrier Syst.* **1999**, *16*, 147–207.
- (4) Hawiger, J. *Curr. Opin. Chem. Biol.* **1999**, *3*, 89–94.
- (5) Lindgren, M.; Hallbrink, M.; Prochiantz, A.; Langel, U. *Trends Pharmacol. Sci.* **2000**, *21*, 99–103.
- (6) Schwarze, S. R.; Hruska, K. A.; Dowdy, S. F. *Trends Cell Biol.* **2000**, *10*, 290–295.
- (7) Wender, P. A.; Mitchell, D. J.; Pattabiraman, K.; Pelkey, E. T.; Steinman, L.; Rothbard, J. B. *Proc. Natl. Acad. Sci. U.S.A.* **2000**, *97*, 13003–13008.
- (8) Umezawa, N.; Gelman, M. A.; Haigis, M. C.; Raines, R. T.; Gellman, S. H. *J. Am. Chem. Soc.* **2002**, *124*, 368–369.
- (9) Zelfhati, O.; Wang, Y.; Kitada, S.; Reed, J. C.; Felgner, P. L.; Corbeil, J. *J. Biol. Chem.* **2001**, *276*, 35103–35110.
- (10) Mukherjee, S.; Ghosh, R. N.; Maxfield, F. R. *Physiol. Rev.* **1997**, *77*, 759–803.
- (11) Mellman, I. *Annu. Rev. Cell Dev. Biol.* **1996**, *12*, 575–625.
- (12) Sandvig, K.; Van Deurs, B. *Annu. Rev. Cell Dev. Biol.* **2002**.
- (13) Merritt, E. A.; Hol, W. G. J. *Cur. Opin. Struct. Biol.* **1995**, *5*, 165–171.
- (14) Hooper, N. M. *Mol. Mem. Biol.* **1999**, *16*, 145–156.
- (15) Brown, D. A.; London, E. *Annu. Rev. Cell Dev. Biol.* **1998**, *14*, 111–136.
- (16) Simons, K.; Ikonen, E. *Nature* **1997**, *387*, 569–572.
- (17) Simons, K.; Ikonen, E. *Science* **2000**, *290*, 1721–1726.
- (18) Simons, K.; Toomre, D. *Nat. Rev. Mol. Cell Biol.* **2000**, *1*, 31–39.
- (19) Kirchhausen, T. *Annu. Rev. Biochem.* **2000**, *69*, 699–727.
- (20) Shogomori, H.; Futerman, A. H. *J. Biol. Chem.* **2001**, *276*, 9182–9188.
- (21) Torgersen, M. L.; Skretting, G.; van Deurs, B.; Sandvig, K. *J. Cell Sci.* **2001**, *114*, 3737–3747.
- (22) Hussey, S. L.; He, E.; Peterson, B. R. *J. Am. Chem. Soc.* **2001**, *123*, 12712–12713.
- (23) Hussey, S. L.; Peterson, B. R. *J. Am. Chem. Soc.* **2002**, *124*, 6265–6273.
- (24) Sampson, N. S.; Mrksich, M.; Bertozzi, C. R. *Proc. Natl. Acad. Sci. U.S.A.* **2001**, *98*, 12870–12871.
- (25) Saxon, E.; Bertozzi, C. R. *Annu. Rev. Cell Dev. Biol.* **2001**, *17*, 1–23.
- (26) Jacobs, C. L.; Yarema, K. J.; Mahal, L. K.; Nauman, D. A.; Charters, N. W.; Bertozzi, C. R. *Methods Enzymol.* **2000**, *327*, 260–275.
- (27) Mahal, L. K.; Yarema, K. J.; Bertozzi, C. R. *Science* **1997**, *276*, 1125–1128.
- (28) Jacobs, C. L.; Goon, S.; Yarema, K. J.; Hinderlich, S.; Hang, H. C.; Chai, D. H.; Bertozzi, C. R. *Biochemistry* **2001**, *40*, 12864–12874.
- (29) Saxon, E.; Bertozzi, C. R. *Science* **2000**, *287*, 2007–2010.
- (30) Hang, H. C.; Bertozzi, C. R. *J. Am. Chem. Soc.* **2001**, *123*, 1242–1243.
- (31) Schmidt, T. G.; Koepke, J.; Frank, R.; Skerra, A. *J. Mol. Biol.* **1996**, *255*, 753–766.
- (32) Martin, S. E.; Peterson, B. R. *J. Pept. Sci.* **2002**, *8*, 227–233.
- (33) Churchill, M. E.; Stura, E. A.; Pinilla, C.; Appel, J. R.; Houghten, R. A.; Kono, D. H.; Balderas, R. S.; Fieser, G. G.; Schulze-Gahmen, U.; Wilson, I. A. *J. Mol. Biol.* **1994**, *241*, 534–556.
- (34) Chen, J.; Skehel, J. J.; Wiley, D. C. *Biochemistry* **1998**, *37*, 13643–13649.
- (35) Korndorfer, I. P.; Skerra, A. *Protein Sci.* **2002**, *11*, 883–893.
- (36) Harris, L. J.; Larson, S. B.; Hasel, K. W.; McPherson, A. *Biochemistry* **1997**, *36*, 1581–1597.

- (37) Deisenhofer, J. *Biochemistry* **1981**, *20*, 2361–2370.
- (38) Mohamadi, F.; Richards, N. G. J.; Guida, W. C.; Liskamp, R.; Lipton, M.; Caufield, C.; Chang, G.; Hendrickson, T.; Still, W. C. *J. Comput. Chem.* **1990**, *11*, 440–467.
- (39) Dubowchik, G. M.; Ditta, J. L.; Herbst, J. J.; Bollini, S.; Vinitzky, A. *Bioorg. Med. Chem. Lett.* **2000**, *10*, 559–562.
- (40) Creaser, S. P.; Peterson, B. R. *J. Am. Chem. Soc.* **2002**, *124*, 2444–2445.
- (41) Heuser, J. E.; Anderson, R. G. W. *J. Cell Biol.* **1989**, *108*, 389–400.
- (42) Wang, L. H.; Rothberg, K. G.; Anderson, R. G. *J. Cell Biol.* **1993**, *123*, 1107–1117.
- (43) Ikonen, E. *Curr. Opin. Cell Biol.* **2001**, *13*, 470–477.
- (44) Leland, P. A.; Staniszewski, K. E.; Kim, B. M.; Raines, R. T. *J. Biol. Chem.* **2001**, *276*, 43095–43102.
- (45) Wardman, P. *Curr. Pharm. Des.* **2002**, *8*, 1363–1374.
- (46) Jacobson, R. H.; Zhang, X. J.; DuBose, R. F.; Matthews, B. W. *Nature* **1994**, *369*, 761–766.

BC025601P